Carbon Nanotube Based Membrane for Light-Driven Simultaneous Proton and Electron Transport

Gregory A. Pilgrim[1], Amanda R. Amori[1], Zhentao Hou[1], Fen Qiu[1], Sanela Lampa-Pastirk[3], and Todd D. Krauss[1,2]

[1]University of Rochester Department of Chemistry and [2]Institute of Optics

[3]Nazareth College Department of Chemistry and Biochemistry

Supporting Information

Table of Contents

Part I: Growth of Vertically Aligned Carbon Nanotube Arrays:

Nanotube arrays were grown on silicon wafers (Ultrasil Corp) purchased with 500 nm of thermal oxide in place. 10 nm of alumina was deposited onto the silicon dioxide layer followed by 1 nm of iron using a Lesker Physical Vapor Deposition system. Chips, roughly 2 cm^2 in in surface area were then removed from larger wafers and introduced, approximately 10 at a time into the sample chamber of a 4" Aixtron Black Magic system. Arrays were grown using the provided "cake" recipe with growth time set to 4 minutes. The resulting nanotube arrays were dense and nominally straight and parallel to one another along the extended axis of the nanotubes (see Figure 2a). Arrays were then fabricated into membranes as described in our previous work[1]

QUES growth_time 1 1800
--- Gases: N2, N2, C2H2, H2
VALV 1 OPEN
WAIT PRES < 0.10
FLOW 1 ON 1000
VALV 1 CLOSE
WAIT PRES > 40.00
TUNE PCON 50mbar 1000sccm N2
PCON ON 50 1
HEAT ON 600.0 300.0
WAIT TEMP > 590.0
FLOW 4 ON 100
FLOW 2 ON 7500
TUNE PCON supergrowth at 720mbar
PCON ON 720 5
WAIT PRES > 715.00
WAIT TIME > 30
HEAT ON 800.0 300.0
FLOW 3 ON 160
SENS IR 500
TUNE HTIR 800C - 700mbar
HEAT ON 720.0 0.0
WAIT TEMP > 720.0
HEAT ON 750.0 100.0

```
WAIT TIME > #growth_time
FLOW 4 OFF
FLOW 2 OFF
FLOW 3 OFF
PCON OFF
HEAT OFF
VALV 1 OPEN
SENS TC 650
FLOW 1 OFF
WAIT PRES < 0.50
FLOW 1 ON 1000
FLOW 2 ON 2000
WAIT TEMP < 600.0
FLOW 2 ON 8000
WAIT TEMP < 400.0
FLOW 2 OFF
FLOW 1 OFF
WAIT PRES < 0.20
```

Part II: Spectroscopic Investigation of Nanotubes

Sample Preparation

SWNT arrays were scraped off of their silicon growth substrate and approximately 0.5mg/mL of the nanotube array material was solubilized in a 1.0% by weight solution of sodium dodecyl sulfate in water. The solution was vortex mixed for one minute (VWR Mini Vortex Mixer), homogenized for 1 hour (Ultra Turrax T8 shear homogenizer), probe sonicated for 1 hour (Branson 450 probe sonicator) using a 1/8" tip, and then ultracentrifuged for 6 hours running at 35,000rpm at 20 °C (Beckman Optima L-90 K ultracentrifuge, SW-41Ti rotor)[2].

Measurements

UV-Vis spectrophotometry as well as photoluminescence (PL) and Raman spectroscopy measurements were performed on the sample solution in a 1cm path length quartz cuvette (Starna Cells, Inc.). The UV-Vis spectrum was acquired using a Lambda

950 UV-Vis-IR spectrophotometer (Perkin Elmer, Inc.) and collected from 1175 nm-200 nm, with a 1nm step size. PL spectra were collected on a home-built fluorometer system with an excitation monochromator (SpectraPro 150, Acton Research Corporation) and an emission monochromator (SpectraPro 300i, Acton Research Corporation) in a right-angle geometry with respect to the sample chamber. Near-infrared emission was detected using a liquid nitrogen cooled InGaAs detector (Electro-Optical Systems, Inc.) Raman spectra were collected on a home-built triple grating setup, using a CCD for detection (Princeton Instruments).

Results

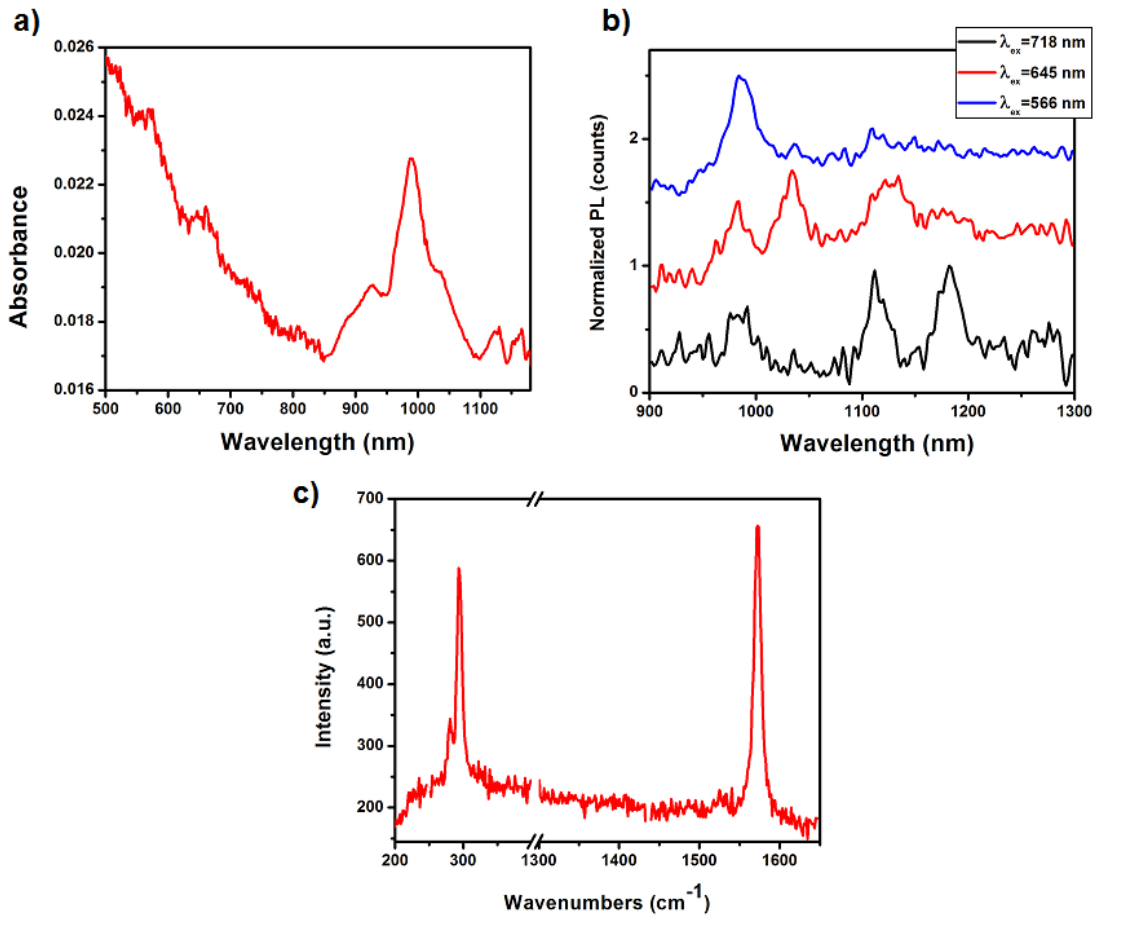

Figure S1: A) UV-vis-IR absorption spectrophotometric evaluation of NT chiralities. Peaks at 984 nm and 567 nm correspond to the E_{11} and E_{22} transitions of (*6*,*5*) NTs.

Similarly peaks at 1022 nm and 643 nm refer to (*7,5*), peaks at 1113 nm and 649 nm refer to (*7,6*), and peaks at 1170 nm and 720 nm refer to (*8,6*). All peaks, and the transitions they mark, have characteristic energies dependent on NT chirality.[3] B) Photoluminescence (PL) spectroscopy measurements of NTs solubilized in sodium dodecyl sulfate at excitation wavelengths of 568 nm, 645 nm, and 718 nm. Spectra are normalized and offset for clarity. Emission can be seen from (*6,5*), (*7,5*), (*7,6*), and (*8,6*) chiralities respectively. C) 660 nm excitation Raman spectroscopy of a sample of NTs solubilized in sodium dodecyl sulfate. The radial breathing mode peaks, at roughly 300 cm^{-1} are characteristic of (*7,6*) and (*7,5*) NTs. For this sample, the G band at 1580 cm^{-1} is quite strong. The D band, expected at roughly 1350 cm^{-1} and associated with defect states, is not observed. The strength of the G band, combined with the lack of D band, indicates the NTs have minimal structural defects.[4]

SWNTs in the membrane were characterized spectroscopically to determine what NT chiralities, and by extension what energy level conduction bands and reduction potentials, were present in membranes. As shown in Figure S1, UV-vis-IR spectrophotometry indicates absorption peaks matching known energy levels of (*6,5*) (*7,5*), (*7,6*), and (*8,6*) NTs, all of which are semiconducting chiralities with among the highest reduction potentials.[5] Because UV-vis-IR spectrophotometry measurements are susceptible to spectral overlap of chiralities, PL and Raman spectroscopies were used to more conclusively identify NT chiralities. Raman spectroscopy confirmed the presence of (*6,5*) (*7,5*) and (*7,6*) SWNTs. PL spectroscopy confirmed the presence of the four previously stated chiralities. PL and Raman measurements do not preclude the possibility of other chiralities of NT also being present, such as those with diameters large enough that they would be excited further to the red than these experiments measured. However, owing to the general mechanism of NT growth from annealed films of metal catalyst it is likely that NTs in a sample would have roughly similar diameters[6] making large diameter, unmeasured tubes unlikely.

Part III: Proton and Electron Crossing Measurements

Simultaneous Crossing

Methyl viologen (at 32 μM) and bromophenol blue (at 4 μM) in water along with an excess of 0.005 moles of ascorbic acid were the two operative solutions in simultaneous crossing experiments (Figure S2). Addition of ascorbic acid to bromophenol blue causes a change from blue to yellow. Yellow color persists, though the solution does visibly darken, over the course of the experiment. Aliquots of bromophenol blue solution were removed and measured spectroscopically every 20 minutes. Aliquots were then returned to the experimental vessel. Methyl viologen and bromophenol blue spectra were both recorded using a Lambda 35 spectrophotometer. To avoid oxygen contamination, to which reduced methyl viologen is very sensitive, methyl viologen spectra were only measured at the beginning and end of the experiment.

Independent Crossing

Proton and electron transport were also evaluated separately. Nanotube membranes were submerged in deionized water for 48 hours prior to crossing experiments to fill the nanotube bores with water.[7] In experiments conducted exactly as those in our previous work on multi walled nanotube membranes,[1] tests of proton transport were performed in glassware similar to that in Figure S2, but with one side filled with a 4 μM solution of bromophenol blue, and the other with 0.1M HCl. A 0.8 V potential was then placed across the system using a Hewlett Packard 6284A DC power supply, with the field oriented as to motivate proton movement from the acid side to the indicator side. The resulting spectral changes in bromophenol blue were monitored spectroscopically and can be seen in Figure S3. To measure electrical conductivity membrane samples were first

coated with 500 nm of gold contact[8] and then their resistance was measured using a Hewlett Packard 4192A Impedance Analyzer. Resistance was then converted to conductivity by inversion and incorporation of sample geometry.

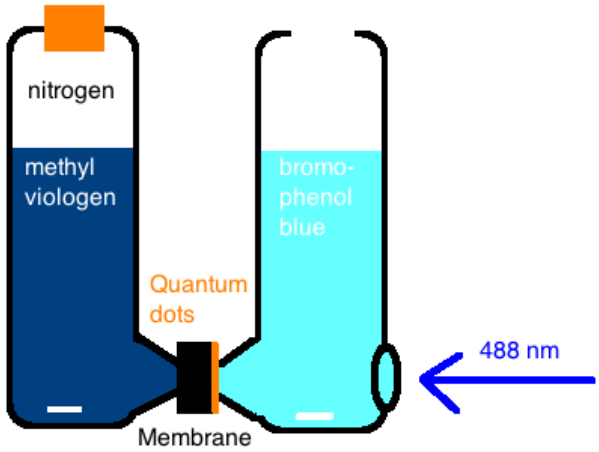

Figure S2: Glassware apparatus for simultaneous proton and electron crossing experiments. One chamber of the glassware apparatus was filled with bromophenol blue (4 μM) in a solution of water and excess ascorbic acid such that the solution was in contact with the quantum dot (QD) coating on the membrane. The other chamber was purged with nitrogen and then filled with a 32 mM solution of methyl viologen (MV) and excess ascorbic acid. A 488 nm continuous wavelength laser was then passed through an expander, to enlarge the laser spot and irradiate a larger membrane area, and into a window on the bromophenol blue-containing glassware side.

Part IV: Proton and Electron Crossing Measurement Analysis

Simultaneous Crossing

The decrease in intensity of the bromophenol blue peak at 449 nm in Figure 3 is caused by both proton migration and photobleaching from the 488 nm laser (Coherent, CW Sapphire LP 488) directed through the solution to photoexcite QDs on the NT membrane. However, the increase in intensity at 595 nm, which is associated with non-protonated bromophenol blue, cannot be the result of bleaching. It reflects only the movement of protons through the NT membrane. The peak at 595 nm can also be observed shifting over time from its initial value to 605 nm. This shift is likely caused by changes in

solution polarity. The peak associated with non-protonated bromophenol blue has been established to exhibit a red shift in the presence of even micromolar amounts of nonpolar species.[9,10] Bleaching of bromophenol blue, a highly conjugated molecule, could result in a lowering of solution polarity and the corresponding red shift seen in Figure 3.

All calculations for electron transfer are based on the 600 nm peak in methyl viologen because the peak at 385 nm (not shown in Figure 3 inset) was almost completely consumed as a result of oxygen exposure. The cuvette itself was sealed and purged with N_2 prior to measurement but some oxygen exposure could occur during transfer of solution between the glassware apparatus and the cuvette. The 600 nm peak was also exposed to some amount of oxygen, however 10-20 mL of MV^{2+} requires approximately 1-2 minutes of exposure to parts per million levels of oxygen to fully transition from its reduced form back to its oxidized form.[11] The length of the spectroscopic scan performed here is roughly two minutes going from red to blue. As such, the peak at 600 nm was exposed to oxygen only very briefly prior to being measured. The peak at 385 nm was exposed for almost two minutes prior to measurement, which accounts for the different peak intensities for each.

Independent Crossing

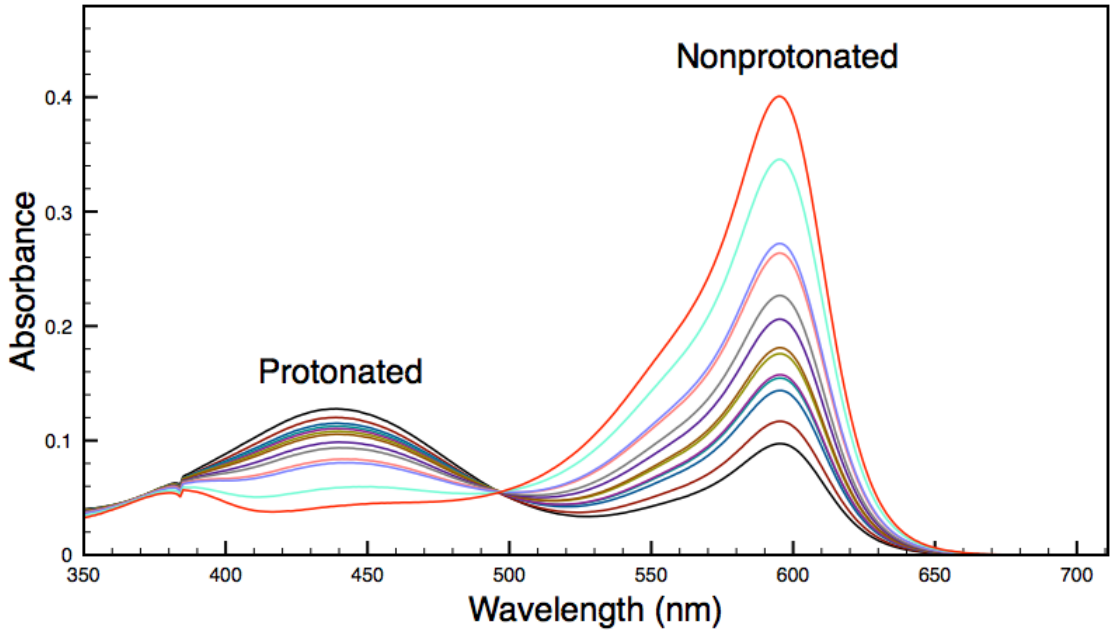

Figure S3: Crossing of protons through a NT membrane assisted by a 0.8 mV potential differenence. The peak at 449 nm associated with protonated bromophenol blue can be seen to increase while that at 595 nm, associated with nonprotonated bromophenol blue decreases. Measurement proceeds from red (zero minutes) to black (180 minutes) in 15 minute intervals. Differences in magnitude of increase/decrease are reflective of the different molar extinction coefficients of the two species.[9]

Control Experiments

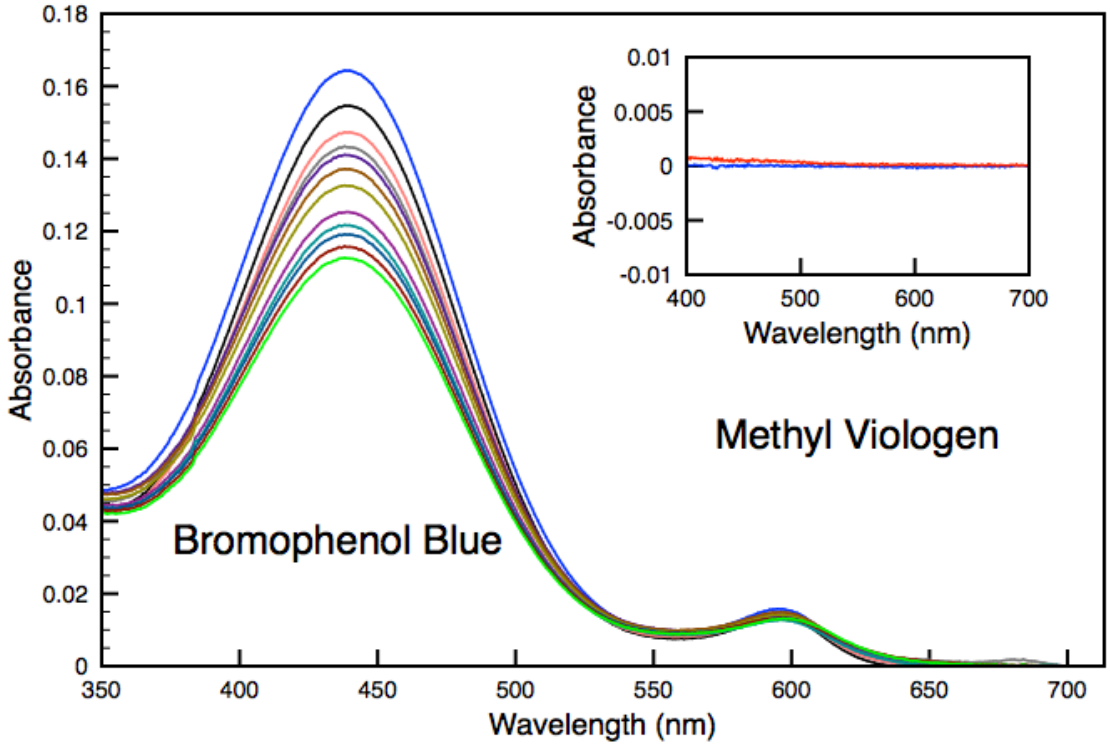

Figure S4: Control experiment wherein simultaneous crossing experiments described in Figure 1 were attempted without QDs. Bromophenol blue spectra shows effects of laser bleaching via the decrease in intensity of the peak at 440 nm from beginning (blue) to end (green) at 15 minute intervals. Changes in solution polarity from bleaching also change the position of the peak at 595 nm, shifting it approximately 10 nm to the red. No increase in intensity is seen at the 595 nm peak, which means there is no movement of protons through the membrane. Inset: Corresponding MV spectra with no change from beginning (blue) to end (red), and therefore no reduction of MV^{2+}.

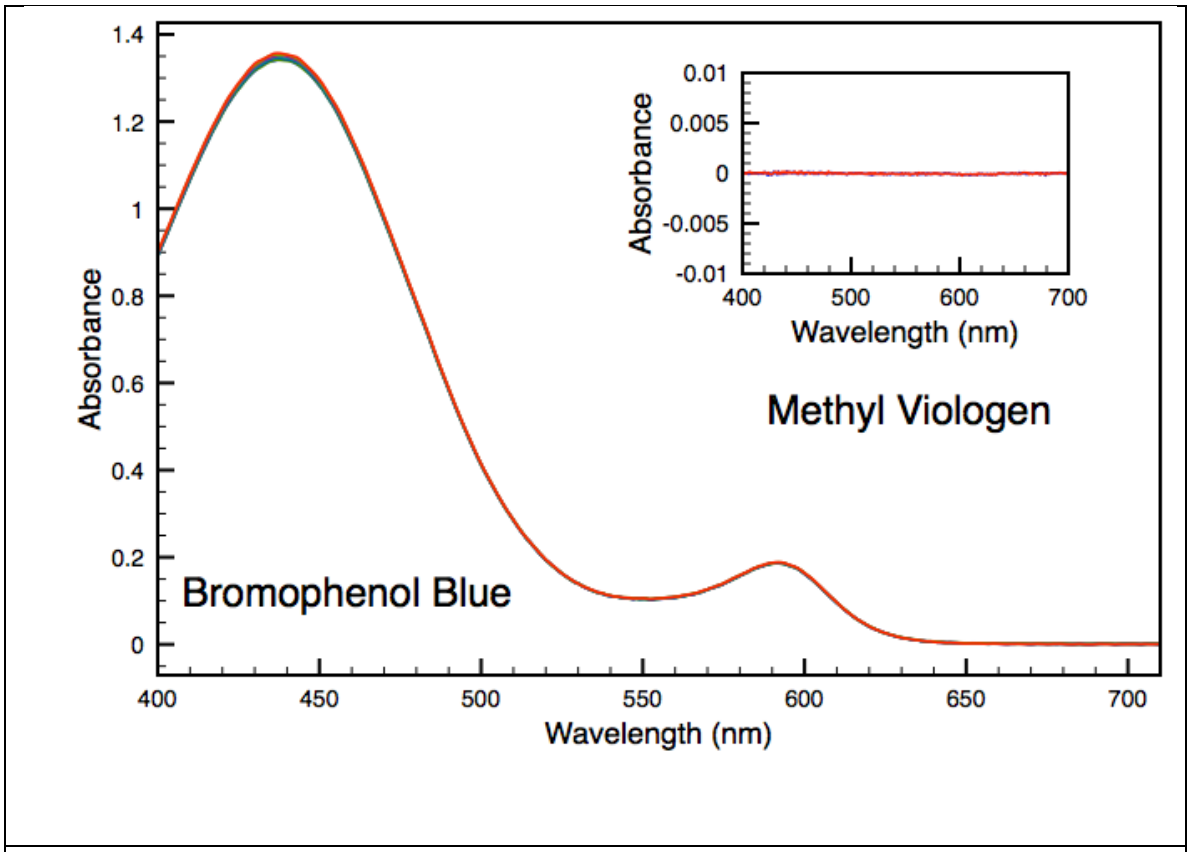

Figure S5: Control experiment wherein simultaneous crossing experiments described in Figure 1 were attempted without laser irradiation. Bromophenol blue spectra displaying no change from beginning (blue) to end (red). Six samples were taken at 20 minute intervals. Inset: MV spectra also showing no change from beginning (blue) to end (red).

Comparison to Existing Literature

Table S1: Comparison Between This Work and Other Published Works

Membrane	**Description**	**Electrical Conductivity**	**Proton Conductivity (Nafion Comparison)**
Javier *et al.*[12]	P3HT-PEO	6.73 µS cm^{-1}	11 mS cm^{-1} (1/8 Nafion)
Liu *et al.*[13]	PEDOT:sPSS	10 S cm^{-1}	20 mS cm^{-1} (1/4 Nafion)
Tortello *et al.*[14]	Multiwalled NTs/Nafion	315 µS cm^{-1}	8.9 mS cm^{-1} (1/9 Nafion)
Spurgeon *et al.*[8]	Silicon nanowire/Nafion/PEDOT	24 mS cm^{-1}	78 mS cm^{-1} (Nafion)
Pilgrim *et al.*[1]	Multiwalled NT based	495 ± 12 mS cm^{-1}	N/A (1/2 Nafion)
Pilgrim *et al.* (current work)	Single walled NT based	558 ± 18 mS cm^{-1}	N/A (15/13 Nafion)

Electrical conductivity of the membrane is also highly competitive, outperforming other published membranes[8,12,14] by orders of magnitude, with the exception of the PEDOT:sPSS membrane developed by Liu *et al.*[13] The Liu membrane uses poly(3,4-ethyl-enedioxythiophene) (PEDOT) as its electrically conductive material and is roughly 20x more conductive than the membranes described in this work. However, Liu *et al.* also found their membrane to have a reduction potential of 380mV vs. SHE, a value completely incompatible with any hydrogen reduction catalyst, even platinum, which has a reduction potential of zero with respect to SHE.[15]

Part V: Intermembrane Reduction Cascade

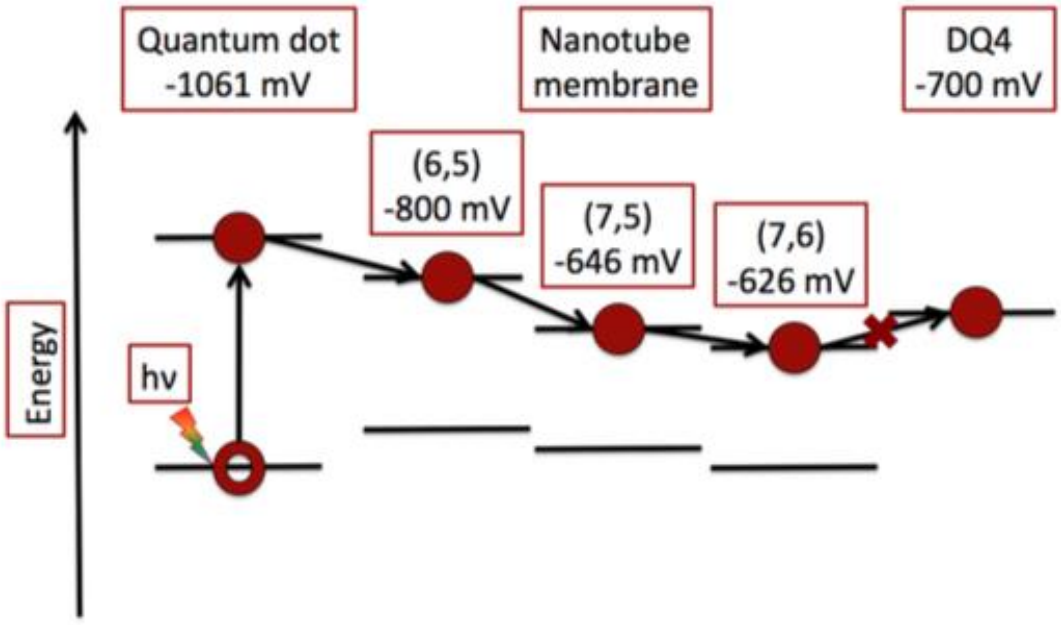

Figure S6: A depiction of the "intermembrane reduction cascade" wherein electrons are transferred from CdSe QDs[16] into the membrane. The overall reduction potential of the NT membrane is that of the species of NT with the least negative reduction potential. In the most optimistic case that NT species is (*7,6*) and the reduction potential is -626 mV (vs. SHE) perhaps explaining the failure of this system to reduce DQ4.[17]

Part VI: References

(1) Pilgrim, G. A.; Leadbetter, J. W.; Qiu, F.; Siitonen, A. J.; Pilgrim, S. M.; Krauss, T. D. Electron Conductive and Proton Permeable Vertically Aligned Carbon Nanotube Membranes. *Nano Lett.* **2014**, *14*, 1728-1733.

(2) Islam, M.; Rojas, E.; Bergey, D.; Johnson, A.; Yodh, A. High weight fraction surfactant solubilization of single-wall carbon nanotubes in water. *Nano Lett.* **2003**, *3*, 269-273.

(3) Weisman, R. B.; Bachilo, S. M. Dependence of Optical Transition Energies on Structure for Single-Walled Carbon Nanotubes in Aqueous Suspension: An Empirical Kataura Plot. *Nano Lett.* **2003**, *3*, 1235-1238.

(4) Jorio, A.; Saito, R.; Hafner, J. H.; Lieber, C. M.; Hunter, M.; McClure, T.; Dresselhaus, G.; Dresselhaus, M. S. Structural (*n*,*m*) Determination of Isolated Single-Wall Carbon Nanotubes by Resonant Raman Scattering. *Phys. Rev. Lett.* **2001**, *86*, 1118-1121.

(5) Paolucci, D.; Franco, M. M.; Iurlo, M.; Marcaccio, M.; Prato, M.; Zerbetto, F.; Pénicaud, A.; Paolucci, F. Singling out the Electrochemistry of Individual Single-Walled Carbon Nanotubes in Solution. *J. Am. Chem. Soc.* **2008**, *130*, 7393-7399.

(6) Zhang, H.; Cao, G.; Wang, Z.; Yang, Y.; Shi, Z.; Gu, Z. Influence of Hydrogen Pretreatment Condition on the Morphology of Fe/Al_2O_3 Catalyst Film and Growth of Millimeter-Long Carbon Nanotube Array. *J. Phys. Chem. C* **2008**, *112*, 4524-4530.

(7) Majumder, M.; Chopra, N.; Andrews, R.; Hinds, B. Nanoscale hydrodynamics - Enhanced flow in carbon nanotubes. *Nature* **2005**, *438*, 44-44.

(8) Spurgeon, J.; Walter, M.; Zhou, J.; Kohl, P.; Lewis, N. Electrical conductivity, ionic conductivity, optical absorption, and gas separation properties of ionically conductive polymer membranes embedded with Si microwire arrays. *Energy Environ. Sci.* **2011**, *4*, 1772-1780.

(9) Bertsch, M.; Mayburd, A.; Kassner, R. The identification of hydrophobic sites on the surface of proteins using absorption difference spectroscopy of bromophenol blue. *Anal. Biochem.* **2003**, *313*, 187-195.

(10) Saikia, P. M.; Dutta, R. K. Effect of Association of Bromophenol Blue with Tween Surfactants on Its Acid-Base Equilibria at High pH. *J. Dispersion Sci. Technol.* **2009**, *30*, 33-37.

(11) Sweetser, P. B. Colorimetric determination of trace levels of oxygen in gases with the photochemically generated methyl viologen radical-cation. *Anal. Chem.* **1967**, *39*, 979-982.

(12) Javier, A.; Patel, S.; Hallinan, D.; Srinivasan, V.; Balsara, N. Simultaneous Electronic and Ionic Conduction in a Block Copolymer: Application in Lithium Battery Electrodes. *Angew. Chem., Int. Ed.* **2011**, *50*, 9848-9851.

(13) Liu, J.; Davis, N.; Liu, D.; Hammond, P. Highly transparent mixed electron and proton conducting polymer membranes. *J. Mater. Chem.* **2012**, *22*, 15534-15539.

(14) Tortello, M.; Bianco, S.; Ijeri, V.; Spinelli, P.; Tresso, E. Nafion membranes with vertically-aligned CNTs for mixed proton and electron conduction. *J. Membr. Sci.* **2012**, *415*, 346-352.

(15) Nič, M. J., J.; Košata, B.; Jenkins, A.; McNaught, A., Eds.; 2.1.0 ed.: In *IUPAC Compendium of Chemical Terminology: Gold Book*; Nič, M. J., J.; Košata, B.; Jenkins, A.; McNaught, A, Ed.; IUPAC: Research Triagle Park, NC, 2009.

(16) Amelia, M.; Avellini, T.; Monaco, S.; Impellizzeri, S.; Yildiz, I.; Raymo, F.; Credi, A. Redox properties of CdSe and CdSe-ZnS quantum dots in solution. *Pure Appl. Chem.* **2011**, *83*, 1-8.

(17) Du, P.; Schneider, J.; Jarosz, P.; Zhang, J.; Brennessel, W.; Eisenberg, R. Photoinduced electron transfer in platinum(II) terpyridyl acetylide chromophores: Reductive and oxidative quenching and hydrogen production. *J. Phys. Chem. B* **2007**, *111*, 6887-6894.